Applied Problems of Nonlinear Oscillation and Wave Theory

Izvestiya Vysshikh Uchebnykh Zavedeniy. Applied Nonlinear Dynamics. 2025;33(4)

Article DOI: 10.18500/0869-6632-003161

Nonlinear dynamics for cylindrical resonator of wave solid-state gyroscope with different number of electrostatic control sensors

A. A. Maslov, D. A. Maslov✉

National Research University "MPEI", Moscow, Russia
E-mail: Maslov954@yandex.ru, ✉MaslovDmA@mpei.ru

Received 18.10.2024, accepted 15.01.2025, available online 29.01.2025, published 31.07.2025

Abstract. The *purpose* of this work is to determine differences in the nonlinearities of mathematical models of dynamics and nonlinear effects of dynamics for the cylindrical resonator of wave solid–state gyroscope using a different number of electrostatic control sensors. *Methods.* In this article resonator oscillations nonlinearity caused by finite ratio of the small deflection of the resonator to the small gap of the electrostatic sensor is considered. To construct approximate mathematical models Tikhonov's theorem on the passage to the limit is used and a small parameter singularly included in the system of differential equations is also taken into account. The equations of resonator dynamics are averaged by using the Krylov–Bogolyubov method. *Results.* The difference between the nonlinear terms in the equations of resonator dynamics with eight and sixteen control sensors is determined. It is found that nonlinear effects are more pronounced in the case of the gyroscope with sixteen control sensors. The angular drift velocity and the displacement of the resonant peak of the amplitude-frequency response are greater than in the case of eight control sensors. It is shown that in the case of eight control sensors, the angular drift velocity has a variable value and also contains a small uncompensated component. *Conclusion.* Mathematical models of the dynamics for the cylindrical resonator of wave solid-state gyroscope taking into account the nonlinearities caused by the excitation of oscillations by eight and sixteen electrostatic control sensors are deduced. The difference between the nonlinear effects of the resonator dynamics for wave solid-state gyroscope with different number of control sensors is shown. The angular drift velocity and the displacement of the resonant peak of the amplitude-frequency response are obtained. Conclusions about the applicability of gyroscope with eight control sensors are discussed.

Keywords: wave solid-state gyroscope, mathematical model, electrostatic sensors, cylindrical resonator, nonlinear oscillations, angular drift velocity.

Acknowledgements. This work was supported by the grant of Russian Science Foundation (project No. 23-21-00546).

For citation: Maslov AA, Maslov DA. Nonlinear dynamics for cylindrical resonator of wave solid-state gyroscope with different number of electrostatic control sensors. Izvestiya VUZ. Applied Nonlinear Dynamics. 2025;33(4):466–484. DOI: 10.18500/0869-6632-003161

Introduction

Improving the accuracy of navigation instruments, including solid-state gyroscopes (SSGs), by developing more accurate mathematical models of their sensitive element dynamics is a pressing issue. Accounting for nonlinear oscillations in mathematical models of SSG resonator dynamics not only improves instrument accuracy through compensation methods, but also allows for the investigation of a number of nonlinear effects that occur in SSG dynamics and cannot be addressed within linear mathematical models.

The foundations of the SSG theory are laid in the works of D. M. Klimov and V. F. Zhuravlev [5–10]. In [6, 9] it is shown that the error caused by the nonlinear properties of the oscillatory system is inherent in all SSGs, and the study of the dynamics can be carried out within the framework of the same equations, similar to the equations of the classical Foucault pendulum. At the same time, it is indicated that the study of nonlinearity requires taking into account the specifics of a particular oscillatory system. In works [11, 12] it is noted that during experimental studies of the dynamics of vibratory gyroscopes with electrostatic control sensors, phenomena characteristic of nonlinear systems were discovered, for example, the breakdown of resonator oscillations. However, little attention has been paid to the study of the specificity of nonlinearity caused by electrostatic control sensors.

This article investigates nonlinear oscillations caused by electrostatic control sensors, derives and compares nonlinear mathematical models with eight and sixteen control sensors, and summarizes the results of previous studies on the nonlinear effects of the dynamics of SSG [13–15], which considered SSGs with only sixteen control sensors.

This article examines a SSG with a cylindrical resonator. This choice is explained by the current intensive work to improve the manufacturing quality and balancing of cylindrical fused quartz resonators [16–20], which differ from hemispherical resonators in their ease of manufacture and relatively high quality factor. The results obtained for a SSG with a cylindrical resonator can be generalized to SSGs with other resonator types: ring and hemispherical.

1. Mathematical models taking into account the nonlinearity of oscillations caused by control sensors

1.1. Mathematical Models for an Arbitrary Number of Control Sensors. We will consider a wave solid-state gyroscope with a cylindrical resonator, one edge of which is free, while the other is rigidly attached to the base of the device. The resonator is made of quartz glass with a metallic coating applied to its surface. The oscillations of the cylindrical resonator are excited by a system of electrostatic control sensors, which are capacitors formed by the metallized surface of the resonator and control electrodes located near the free edge of the resonator. A mathematical model of the cylindrical resonator dynamics for this type of wave solid-state gyroscope is developed in detail in [14]. In general, for an arbitrary number of control sensors, the mathematical model has the form

$$\begin{aligned} &\ddot{f} + \omega^2 f = -\gamma\dot{f} + 2v\dot{g} + \frac{1}{2md^2C_0}\sum_{j=1}^{n} q_j^2 \cos 2\theta_j, \\ &\ddot{g} + \omega^2 g = -\gamma\dot{g} - 2v\dot{f} + \frac{1}{2md^2C_0}\sum_{j=1}^{n} q_j^2 \sin 2\theta_j, \end{aligned} \tag{1}$$

$$R_e C_0 \dot{q}_j + q_j\,(1 - f\cos 2\theta_j - g\sin 2\theta_j) = U_j u_0 C_0, \quad j = 1\ldots n. \tag{2}$$

where, in accordance with [14], the following are designated: $f(t)$, $g(t)$ — generalized coordinates of the second mode of oscillation of the cylindrical resonator, normalized by the gap d between the control electrode and the undeformed resonator; ω — characteristic frequency of natural oscillations; γ characterizes the damping of oscillations; v characterizes the angular velocity of rotation of the gyroscope; m — reduced mass of the cylindrical resonator; C_0 — capacitance of capacitors with an undeformed resonator; $q_j(t)$ — charge of the j-th capacitor formed by the resonator and the j-th control electrode; $\theta_j = 2\pi(j-1)/n$ — angle of the j-th electrode, $j = 1\ldots n$, n — number of control electrodes; R_e — electrical resistance of

the oscillation control circuit; $U_j(t)$ — voltage on the j-th electrode, $j = 1 \dots n$, which is normalized by the value of the constant reference voltage u_0. The dot denotes differentiation with respect to time t.

Let us move in equations (1), (2) to the dimensionless time $\tau = \omega t$ and charges $Q_j = q_j/(C_0 u_0)$ normalized by the quantity $Q_0 = C_0 u_0$:

$$\begin{aligned} &\frac{\mathrm{d}^2 f}{\mathrm{d}\tau^2} + f + \tilde{\gamma}\frac{\mathrm{d}f}{\mathrm{d}\tau} - \tilde{v}\frac{\mathrm{d}g}{\mathrm{d}\tau} - \frac{\eta}{8}\sum_{j=1}^{n} Q_j^2 \cos 2\theta_j = 0, \\ &\frac{\mathrm{d}^2 g}{\mathrm{d}\tau^2} + g + \tilde{\gamma}\frac{\mathrm{d}g}{\mathrm{d}\tau} + \tilde{v}\frac{\mathrm{d}f}{\mathrm{d}\tau} - \frac{\eta}{8}\sum_{j=1}^{n} Q_j^2 \sin 2\theta_j = 0, \end{aligned} \tag{3}$$

$$\varepsilon\frac{\mathrm{d}Q_j}{\mathrm{d}\tau} + Q_j\left(1 - f\cos 2\theta_j - g\sin 2\theta_j\right) = U_j, \quad j = 1 \dots n, \tag{4}$$

where $\eta = \dfrac{C_0^2 u_0^2}{2md^2\omega^2}$, $\varepsilon = R_e C_0 \omega$ are dimensionless small parameters, and dimensionless small quantities $\tilde{\gamma} = \gamma/\omega$, $\tilde{v} = v/\omega$ are also denoted. Note that the small parameter $\varepsilon = R_e C_0 \omega$ characterizes the ratio of the active and reactive (capacitive) resistances of the oscillation control circuit and is extremely small for electrostatic sensors, for example, $\varepsilon \approx 10^{-8}$ for $R_e \approx 1$ Ohm, $C_0 \approx 10^{-12}$ F, $\omega \approx 10^4$ s^{-1}.

The presence of the small parameter ε in the derivatives indicates that the equations (4) are singularly perturbed, and the entire system of equations (3), (4) belongs to the class of Tikhonov systems of differential equations. In [14] the application of Tikhonov's theorem on limit transition is shown, which guarantees the approximation of the solution of equations (3) by the solution of equations

$$\frac{\mathrm{d}^2 f}{\mathrm{d}\tau^2} + f = -\tilde{\gamma}\frac{\mathrm{d}f}{\mathrm{d}\tau} + \tilde{v}\frac{\mathrm{d}g}{\mathrm{d}\tau} + \frac{\eta}{8}\sum_{j=1}^{n}\frac{U_j^2\cos 2\theta_j}{\left(1 - f\cos 2\theta_j - g\sin 2\theta_j\right)^2}, \tag{5}$$

$$\frac{\mathrm{d}^2 g}{\mathrm{d}\tau^2} + g = -\tilde{\gamma}\frac{\mathrm{d}g}{\mathrm{d}\tau} - \tilde{v}\frac{\mathrm{d}f}{\mathrm{d}\tau} + \frac{\eta}{8}\sum_{j=1}^{n}\frac{U_j^2\sin 2\theta_j}{\left(1 - f\cos 2\theta_j - g\sin 2\theta_j\right)^2}. \tag{6}$$

However, it is possible to construct a more refined approximation to the solution of equations (1) that takes into account the small parameter ε, which characterizes the parameters of the electric control circuit. Similar to [15], we use a first-order approximation in ε for the variables Q_j, $j = 1 \dots n$, and write a mathematical model of the resonator dynamics that takes into account the parameters of the electric control circuit:

$$\begin{aligned} \frac{\mathrm{d}^2 f}{\mathrm{d}\tau^2} + f = -\tilde{\gamma}\frac{\mathrm{d}f}{\mathrm{d}\tau} + \tilde{v}\frac{\mathrm{d}g}{\mathrm{d}\tau} + \frac{\eta}{8}\Bigg[&\sum_{j=1}^{n}\frac{U_j^2\cos 2\theta_j}{\left(1 - w_j\right)^2} - \\ &-2\varepsilon\sum_{j=1}^{n}\frac{U_j\cos 2\theta_j}{\left(1 - w_j\right)^3}\frac{\mathrm{d}U_j}{\mathrm{d}\tau} - 2\varepsilon\sum_{j=1}^{n}\frac{U_j^2\cos 2\theta_j}{\left(1 - w_j\right)^4}\left(\frac{\mathrm{d}f}{\mathrm{d}\tau}\cos 2\theta_j + \frac{\mathrm{d}g}{\mathrm{d}\tau}\sin 2\theta_j\right)\Bigg], \end{aligned} \tag{7}$$

$$\begin{aligned} \frac{\mathrm{d}^2 g}{\mathrm{d}\tau^2} + g = -\tilde{\gamma}\frac{\mathrm{d}g}{\mathrm{d}\tau} - \tilde{v}\frac{\mathrm{d}f}{\mathrm{d}\tau} + \frac{\eta}{8}\Bigg[&\sum_{j=1}^{n}\frac{U_j^2\sin 2\theta_j}{\left(1 - w_j\right)^2} - \\ &-2\varepsilon\sum_{j=1}^{n}\frac{U_j\sin 2\theta_j}{\left(1 - w_j\right)^3}\frac{\mathrm{d}U_j}{\mathrm{d}\tau} - 2\varepsilon\sum_{j=1}^{n}\frac{U_j^2\sin 2\theta_j}{\left(1 - w_j\right)^4}\left(\frac{\mathrm{d}f}{\mathrm{d}\tau}\cos 2\theta_j + \frac{\mathrm{d}g}{\mathrm{d}\tau}\sin 2\theta_j\right)\Bigg], \end{aligned} \tag{8}$$

where, to shorten the notation, the resonator deflection is denoted as $w_j = f\cos 2\theta_j + g\sin 2\theta_j$.

Obviously, (5), (6) follow from (7), (8) for $\varepsilon = 0$. We will use the presented mathematical models to study the nonlinearity of resonator oscillations caused by electrostatic control sensors with different numbers of control sensors.

1.2. Nonlinear mathematical model of the dynamics of a SSG resonator using eight control sensors. We will consider a case commonly encountered in SSG designs, in which the voltages U_j between the j-th control sensor electrode and the resonator, $j = 1 \dots n$, are applied to eight, $n = 8$, control sensors, all oriented in a fixed manner relative to the SSG base, $\theta_j = (j-1)\pi/4$:

$$\begin{aligned} U_1 = U_5 &= 1 + u_A = 1 - u_1 \sin \mu\tau + u_2 \cos \mu\tau, \\ U_3 = U_7 &= 1 - u_A = 1 + u_1 \sin \mu\tau - u_2 \cos \mu\tau, \\ U_2 = U_6 &= 1 + u_B = 1 - u_3 \sin \mu\tau + u_4 \cos \mu\tau, \\ U_4 = U_8 &= 1 - u_B = 1 + u_3 \sin \mu\tau - u_4 \cos \mu\tau, \end{aligned} \tag{9}$$

where u_1, u_2, u_3, u_4 are the control voltage amplitudes normalized with respect to the reference voltage, u_0, $|u_i| < 1$, $i = 1 \dots 4$; $u_A(\tau)$, $u_B(\tau)$ — normalized control voltages applied respectively to the group of electrodes No. 1, 3, 5, 7 and to an angle offset relative to them 45° group of electrodes No. 2, 4, 6, 8. The value $\mu = \omega_0/\omega = (\omega + \lambda)/\omega$ is introduced, where ω_0 is the frequency of external harmonic excitation of resonator oscillations close to ω, λ — frequency tuning, $|\lambda| \ll \omega$.

The control signals (9) implement the supply of the potential difference $u_0(1+u)$ and $u_0(1-u)$ to the sensors located orthogonally, which is used to linearize the force of the electrostatic sensor, proportional to the square of the voltage on the electrode:

$$u_0^2(1+u)^2 - u_0^2(1-u)^2 = 4u_0^2 u. \tag{10}$$

The resulting expression (10) is linear with respect to the normalized control voltage u.This implements the "push-pull" control scheme widely used in SSGs [6]. Since the electrostatic force is inversely proportional to the square of the gap between the control electrode and the metallized surface of the resonator, we will show that taking into account the finite ratio of the resonator deflection to the gap of the electrostatic sensor violates the "push-pull" linearization. Despite the finite ratio of the deflection to the gap, the magnitude of the deflection is small, which justifies the simultaneous use of linear shell theory and the nonlinearity of the force action of the control sensor in deriving the equations of resonator dynamics. The force action of two orthogonally located control sensors is proportional to an expression that can be expanded in a series according to the deflection normalized by the gap value $|w| < 1$:

$$\begin{aligned} &\frac{u_0^2(1+u)^2}{(1-w)^2} - \frac{u_0^2(1-u)^2}{(1+w)^2} = \\ &\quad = u_0^2(1+u)^2\left(1 + 2w + 3w^2 + 4\tilde{w}^3 + \dots\right) - u_0^2(1-u)^2\left(1 - 2w + 3w^2 - 4w^3 + \dots\right) = \\ &\quad\quad = 4u_0^2 u\left(1 + 3w^2 + 5w^4 + \dots\right) + 4u_0^2\left(1 + u^2\right)\left(w + 2w^3 + 3w^5 + \dots\right) = \\ &\quad\quad\quad = 4u_0^2\left(u + w + u^2 w + 3uw^2 + 2w^3 + 2u^2 w^3 + \dots\right). \end{aligned} \tag{11}$$

Thus, when taking into account the deflection w, the "push-pull" linearization scheme is violated. Neglecting the deflection if it is small, we obtain from (11) a linear expression with respect to the control voltage, corresponding to the "push-pull" linearization (10).

To transform the sums in (7), (8) we will also use series expansions

$$\begin{aligned} \frac{1}{(1-\tilde{w})^2} &= \frac{1}{2}\sum_{k=0}^{\infty}(k+1)\tilde{w}^k = 1 + 2\tilde{w} + 3\tilde{w}^2 + 4\tilde{w}^3 + \dots, \\ \frac{1}{(1-\tilde{w})^3} &= \frac{1}{2}\sum_{k=0}^{\infty}(k+2)(k+1)\tilde{w}^k = 1 + 3\tilde{w} + 6\tilde{w}^2 + 10\tilde{w}^3 + \dots, \\ \frac{1}{(1-\tilde{w})^4} &= \frac{1}{6}\sum_{k=0}^{\infty}(k+3)(k+2)(k+1)\tilde{w}^k = 1 + 4\tilde{w} + 10\tilde{w}^2 + 20\tilde{w}^3 + \dots \end{aligned} \tag{12}$$

Using in (7), (8) the law of voltage supply (9), the approximation (11), the series expansion (12) and neglecting nonlinear terms above the third degree, we obtain the following equations of the resonator dynamics for $n = 8$ control sensors:

$$\begin{aligned}\frac{\mathrm{d}^2 f}{\mathrm{d}\tau^2} + f = -\tilde{\gamma}\frac{\mathrm{d}f}{\mathrm{d}\tau} + \tilde{v}\frac{\mathrm{d}g}{\mathrm{d}\tau} + \eta\left(f + 2f^3 - \varepsilon\left(1 + 10f^2\right)\frac{\mathrm{d}f}{\mathrm{d}\tau} + \right.\\ \left. + \left(1 + 3f^2 - 8\varepsilon f\frac{\mathrm{d}f}{\mathrm{d}\tau}\right)u_A - \varepsilon\left(1 + 6f^2\right)u_A'\right),\\ \frac{\mathrm{d}^2 g}{\mathrm{d}\tau^2} + g = -\tilde{\gamma}\frac{\mathrm{d}g}{\mathrm{d}\tau} - \tilde{v}\frac{\mathrm{d}f}{\mathrm{d}\tau} + \eta\left(g + 2g^3 - \varepsilon\left(1 + 10g^2\right)\frac{\mathrm{d}g}{\mathrm{d}\tau} + \right.\\ \left. + \left(1 + 3g^2 - 8\varepsilon g\frac{\mathrm{d}g}{\mathrm{d}\tau}\right)u_B - \varepsilon\left(1 + 6g^2\right)u_B'\right).\end{aligned} \tag{13}$$

In equations (13) and further, we neglect the terms containing u_A^2 and u_B^2 due to their smallness. Such terms characterize the parametric excitation of the resonator oscillations accompanying the forced oscillations [14]. The stability of oscillations under this accompanying parametric excitation was studied in [21].

To study nonlinear dynamics effects, we need the averaged equations for the SSG resonator dynamics.

First, let us consider (13) for the case $\varepsilon = 0$:

$$\begin{aligned}\frac{\mathrm{d}^2 f}{\mathrm{d}\tau^2} + f = -\tilde{\gamma}\frac{\mathrm{d}f}{\mathrm{d}\tau} + \tilde{v}\frac{\mathrm{d}g}{\mathrm{d}\tau} + \eta\left(f + 2f^3 + \left(1 + 3f^2\right)u_A\right),\\ \frac{\mathrm{d}^2 g}{\mathrm{d}\tau^2} + g = -\tilde{\gamma}\frac{\mathrm{d}g}{\mathrm{d}\tau} - \tilde{v}\frac{\mathrm{d}f}{\mathrm{d}\tau} + \eta\left(g + 2g^3 + \left(1 + 3g^2\right)u_B\right).\end{aligned} \tag{14}$$

And we will carry out averaging of the system of equations (14) using the Krylov–Bogolyubov method [22].

Using variable substitution

$$x_1 = f, \quad x_2 = \frac{\mathrm{d}f}{\mathrm{d}\tau}, \quad x_3 = g, \quad x_4 = \frac{\mathrm{d}g}{\mathrm{d}\tau} \tag{15}$$

Let us reduce (14) to a normal system of differential equations:

$$\begin{aligned}\frac{\mathrm{d}x_1}{\mathrm{d}\tau} &= x_2,\\ \frac{\mathrm{d}x_2}{\mathrm{d}\tau} &= -x_1 - \tilde{\gamma}x_2 + \tilde{v}x_4 + \eta\left(x_1 + 2x_1^3 + \left(1 + 3x_1^2\right)u_A\right),\\ \frac{\mathrm{d}x_3}{\mathrm{d}\tau} &= x_4,\\ \frac{\mathrm{d}x_4}{\mathrm{d}\tau} &= -x_3 - \tilde{\gamma}x_4 - \tilde{v}x_2 + \eta\left(x_3 + 2x_3^3 + \left(1 + 3x_3^2\right)u_B\right).\end{aligned} \tag{16}$$

Using change of variables

$$\begin{aligned}x_1 = p_1\sin\mu\tau + q_1\cos\mu\tau, \quad x_2 = \mu\left(p_1\cos\mu\tau - q_1\sin\mu\tau\right),\\ x_3 = p_2\sin\mu\tau + q_2\cos\mu\tau, \quad x_4 = \mu\left(p_2\cos\mu\tau - q_2\sin\mu\tau\right),\end{aligned} \tag{17}$$

we derive from (16) a system of differential equations resolved with respect to derivatives, which we write in abbreviated vector-matrix form

$$\frac{\mathrm{d}\mathbf{z}}{\mathrm{d}\tau} = F(\mathbf{z}, \tau), \tag{18}$$

where $\mathbf{z}(\tau) = (q_1(\tau), p_1(\tau), q_2(\tau), p_2(\tau))^T$, the function $F(\mathbf{z}, \tau)$ is periodic in τ with period $2\pi/\mu$. Carrying out averaging (18) over the explicitly entering dimensionless time τ, we arrive at a system whose solution gives an approximation to the solution (18), justified by the Krylov–Bogolyubov averaging method [22]:

$$\frac{d\bar{\mathbf{z}}}{d\tau} = \overline{\mathbf{F}}(\bar{\mathbf{z}}). \tag{19}$$

Next, we will omit the notation for the averaged solution and write (19) in the form

$$\begin{aligned}
\frac{dq_1}{d\tau} &= \frac{1}{2}\left[-2p_1\mu - q_1\tilde{\gamma} + q_2\tilde{v} + \eta\left(3k_1 + (1+k_5)\,u_1 + 3k_9u_2\right)\right],\\
\frac{dp_1}{d\tau} &= \frac{1}{2}\left[2q_1\mu - p_1\tilde{\gamma} + p_2\tilde{v} + \eta\left(3k_2 + (1+k_6)\,u_2 + 3k_9u_1\right)\right],\\
\frac{dq_2}{d\tau} &= \frac{1}{2}\left[-2p_2\mu - q_2\tilde{\gamma} - q_1\tilde{v} + \eta\left(3k_3 + (1+k_7)\,u_3 + 3k_{10}u_4\right)\right],\\
\frac{dp_2}{d\tau} &= \frac{1}{2}\left[2q_2\mu - p_2\tilde{\gamma} - p_1\tilde{v} + \eta\left(3k_4 + (1+k_8)\,u_4 + 3k_{10}u_3\right)\right],
\end{aligned} \tag{20}$$

where the notations for nonlinear terms are introduced:

$$\begin{aligned}
k_1 &= -p_1\left(q_1^2 + p_1^2\right)/2, \quad k_2 = q_1\left(q_1^2 + p_1^2\right)/2,\\
k_3 &= -p_2\left(q_2^2 + p_2^2\right)/2, \quad k_4 = q_2\left(q_2^2 + p_2^2\right)/2,
\end{aligned} \tag{21}$$

as well as nonlinearities in control voltages:

$$\begin{gathered}
k_5 = 3\left(3p_1^2 + q_1^2\right)/4, \quad k_6 = 3\left(p_1^2 + 3q_1^2\right)/4, \quad k_7 = 3\left(3p_2^2 + q_2^2\right)/4,\\
k_8 = 3\left(p_2^2 + 3q_2^2\right)/4, \quad k_9 = -q_1p_1/2, \quad k_{10} = -q_2p_2/2.
\end{gathered} \tag{22}$$

Carrying out averaging of equations (13) using the Krylov–Bogolyubov method with $\varepsilon \neq 0$ and the absence of control actions $u_1 = u_2 = u_3 = u_4 = 0$ similarly to the algorithm described above (15)–(19), we obtain the averaged system

$$\begin{aligned}
\frac{dq_1}{d\tau} &= \frac{1}{2}\left[-q_1\tilde{\gamma} + q_2\tilde{v} + \eta\left(3k_1 - 5\varepsilon k_2\right)\right],\\
\frac{dp_1}{d\tau} &= \frac{1}{2}\left[-p_1\tilde{\gamma} + p_2\tilde{v} + \eta\left(3k_2 + 5\varepsilon k_1\right)\right],\\
\frac{dq_2}{d\tau} &= \frac{1}{2}\left[-q_2\tilde{\gamma} - q_1\tilde{v} + \eta\left(3k_3 - 5\varepsilon k_4\right)\right],\\
\frac{dp_2}{d\tau} &= \frac{1}{2}\left[-p_2\tilde{\gamma} - p_1\tilde{v} + \eta\left(3k_4 + 5\varepsilon k_3\right)\right],
\end{aligned} \tag{23}$$

which we will further use to study the angular velocity of the SSG drift.

1.3. Nonlinear mathematical model of the dynamics of the SSG resonator using sixteen control sensors. Let us consider the case in which the voltages U_j between the j-th electrode of the control sensor and the resonator, $j = 1, \ldots, n$, are supplied to sixteen, $n = 16$, control sensors, which are invariably oriented relative to the base of the SSG, $\theta_j = (j-1)\pi/8$:

$$\begin{aligned}
U_1 = U_9 &= 1 + u_A = 1 - u_1\sin\mu\tau + u_2\cos\mu\tau,\\
U_5 = U_{13} &= 1 - u_A = 1 + u_1\sin\mu\tau - u_2\cos\mu\tau,\\
U_3 = U_{11} &= 1 + u_B = 1 - u_3\sin\mu\tau + u_4\cos\mu\tau,\\
U_7 = U_{15} &= 1 - u_B = 1 + u_3\sin\mu\tau - u_4\cos\mu\tau,
\end{aligned} \tag{24}$$

where $u_A(t)$, $u_B(t)$ are normalized control voltages applied respectively to the group of electrodes № 1, 5, 9, 13 and the group of electrodes № 3, 7, 11, 15 shifted relative to them by an angle of 45°. At the

intermediate electrodes (with even numbers), the potential difference is set equal to the reference voltage u_0. The remaining designations are introduced in the same way as in (9).

Using in (7), (8) the law of voltage supply (24), the approximation (11), the series expansion (12) and neglecting nonlinear terms above the third degree, we obtain the following equations of the resonator dynamics for $n = 16$ control sensors [15]:

$$\begin{aligned}
\frac{\mathrm{d}^2 f}{\mathrm{d}\tau^2} + f = &-\tilde{\gamma}\frac{\mathrm{d}f}{\mathrm{d}\tau} + \tilde{v}\frac{\mathrm{d}g}{\mathrm{d}\tau} + \eta\left(2f + 3\left(f^2+g^2\right)f + \left(1 + 3f^2 - 8\varepsilon f\frac{\mathrm{d}f}{\mathrm{d}\tau}\right)u_A\right) - \\
&- \varepsilon\eta\left(2\frac{\mathrm{d}f}{\mathrm{d}\tau} + 5\left(f^2+g^2\right)\frac{\mathrm{d}f}{\mathrm{d}\tau} + 10\left(f\frac{\mathrm{d}f}{\mathrm{d}\tau} + g\frac{\mathrm{d}g}{\mathrm{d}\tau}\right)f + \left(1+6f^2\right)u'_A\right), \\
\frac{\mathrm{d}^2 g}{\mathrm{d}\tau^2} + g = &-\tilde{\gamma}\frac{\mathrm{d}g}{\mathrm{d}\tau} - \tilde{v}\frac{\mathrm{d}f}{\mathrm{d}\tau} + \eta\left(2g + 3\left(f^2+g^2\right)g + \left(1 + 3g^2 - 8\varepsilon g\frac{\mathrm{d}g}{\mathrm{d}\tau}\right)u_B\right) - \\
&- \varepsilon\eta\left(2\frac{\mathrm{d}g}{\mathrm{d}\tau} + 5\left(f^2+g^2\right)\frac{\mathrm{d}g}{\mathrm{d}\tau} + 10\left(f\frac{\mathrm{d}f}{\mathrm{d}\tau} + g\frac{\mathrm{d}g}{\mathrm{d}\tau}\right)g + \left(1+6g^2\right)u'_B\right).
\end{aligned} \tag{25}$$

First, let us consider (25) in the case $\varepsilon = 0$:

$$\begin{aligned}
\frac{\mathrm{d}^2 f}{\mathrm{d}\tau^2} + f &= -\tilde{\gamma}\frac{\mathrm{d}f}{\mathrm{d}\tau} + \tilde{v}\frac{\mathrm{d}g}{\mathrm{d}\tau} + \eta\left(2f + 3\left(f^2+g^2\right)f + \left(1+3f^2\right)u_A\right), \\
\frac{\mathrm{d}^2 g}{\mathrm{d}\tau^2} + g &= -\tilde{\gamma}\frac{\mathrm{d}g}{\mathrm{d}\tau} - \tilde{v}\frac{\mathrm{d}f}{\mathrm{d}\tau} + \eta\left(2g + 3\left(f^2+g^2\right)g + \left(1+3g^2\right)u_B\right),
\end{aligned} \tag{26}$$

and we write out the corresponding (26) averaged equations of the dynamics of the SSG resonator:

$$\begin{aligned}
\frac{\mathrm{d}q_1}{\mathrm{d}\tau} &= \frac{1}{2}\left[-2p_1\mu - q_1\tilde{\gamma} + q_2\tilde{v} + \eta\left(3\tilde{k}_1 + \left(1+k_5\right)u_1 + 3k_9u_2\right)\right], \\
\frac{\mathrm{d}p_1}{\mathrm{d}\tau} &= \frac{1}{2}\left[2q_1\mu - p_1\tilde{\gamma} + p_2\tilde{v} + \eta\left(3\tilde{k}_2 + \left(1+k_6\right)u_2 + 3k_9u_1\right)\right], \\
\frac{\mathrm{d}q_2}{\mathrm{d}\tau} &= \frac{1}{2}\left[-2p_2\mu - q_2\tilde{\gamma} - q_1\tilde{v} + \eta\left(3\tilde{k}_3 + \left(1+k_7\right)u_3 + 3k_{10}u_4\right)\right], \\
\frac{\mathrm{d}p_2}{\mathrm{d}\tau} &= \frac{1}{2}\left[2q_2\mu - p_2\tilde{\gamma} - p_1\tilde{v} + \eta\left(3\tilde{k}_4 + \left(1+k_8\right)u_4 + 3k_{10}u_3\right)\right],
\end{aligned} \tag{27}$$

where the notations for nonlinear terms are introduced similarly to [14]:

$$\begin{gathered}
\tilde{k}_1 = -p_1E - q_2X, \quad \tilde{k}_2 = q_1E - p_2X, \quad \tilde{k}_3 = -p_2E + q_1X, \quad \tilde{k}_4 = q_2E + p_1X, \\
E = 3\left(q_1^2 + p_1^2 + q_2^2 + p_2^2\right)/4, \quad X = \left(p_2q_1 - p_1q_2\right)/2,
\end{gathered} \tag{28}$$

nonlinearities at control voltages have the form (22).

The case of $n = 16$ electrostatic control sensors with $\varepsilon = 0$ was studied in more detail in [14], and for $\varepsilon \neq 0$ — in [15].

For $\varepsilon \neq 0$ and the absence of control actions $u_1 = u_2 = u_3 = u_4 = 0$, an averaged system can be obtained [15]:

$$\begin{aligned}
\frac{\mathrm{d}q_1}{\mathrm{d}\tau} &= \frac{1}{2}\left[-q_1\tilde{\gamma} + q_2\tilde{v} + \eta\left(3\tilde{k}_1 - 5\varepsilon\tilde{k}_2\right)\right], \\
\frac{\mathrm{d}p_1}{\mathrm{d}\tau} &= \frac{1}{2}\left[-p_1\tilde{\gamma} + p_2\tilde{v} + \eta\left(3\tilde{k}_2 + 5\varepsilon\tilde{k}_1\right)\right], \\
\frac{\mathrm{d}q_2}{\mathrm{d}\tau} &= \frac{1}{2}\left[-q_2\tilde{\gamma} - q_1\tilde{v} + \eta\left(3\tilde{k}_3 - 5\varepsilon\tilde{k}_4\right)\right], \\
\frac{\mathrm{d}p_2}{\mathrm{d}\tau} &= \frac{1}{2}\left[-p_2\tilde{\gamma} - p_1\tilde{v} + \eta\left(3\tilde{k}_4 + 5\varepsilon\tilde{k}_3\right)\right],
\end{aligned} \tag{29}$$

which we will further use to study the angular velocity of the SSG drift.

Also, note from equations (20) and (25) that the difference is observed only for cubic nonlinearities; the nonlinearities for control voltages are the same whether eight or sixteen control electrodes are used.

2. Study of nonlinear effects of the SSG resonator dynamics

In this section, we will derive the nonlinear effects of the dynamics of a cylindrical resonator with eight control sensors and compare the obtained results with the results obtained earlier in [14] and [15] for a SSG with sixteen electrostatic control sensors.

2.1. Angular drift velocity. Let us consider the effect of nonlinearity caused by applying a reference voltage to the control sensors on the angular velocity of the gyroscope drift. Let only a constant reference voltage $U_0 \neq 0$ be applied to the control electrodes, and the control voltages $u_1 = u_2 = u_3 = u_4 = 0$.

We will study the drift of the SSG using variables called orbital elements [9]: $r(\tau)$ and $k(\tau)$ are the amplitudes of the fundamental and quadrature oscillation waves, $\theta(\tau)$ is the precession angle, $\chi(\tau)$ is the time phase,

$$\begin{aligned} x_1 &= r\cos(\tau+\chi)\cos 2\theta - k\sin(\tau+\chi)\sin 2\theta, \\ x_3 &= r\cos(\tau+\chi)\sin 2\theta + k\sin(\tau+\chi)\cos 2\theta. \end{aligned} \tag{30}$$

Equations (23) are obtained by averaging the equations of the dynamics of a SSG resonator with $n = 8$ control sensors (13) for $u_1 = u_2 = u_3 = u_4 = 0$. To go from $q_1(\tau)$, $p_1(\tau)$, $q_2(\tau)$, $p_2(\tau)$ to $r(\tau)$, $k(\tau)$, $\theta(\tau)$, $\chi(\tau)$, we will use the change of variables [23]

$$\begin{aligned} q_1 &= r\cos 2\theta\cos\chi - k\sin 2\theta\sin\chi, \qquad & p_1 &= -r\cos 2\theta\sin\chi - k\sin 2\theta\cos\chi, \\ q_2 &= r\sin 2\theta\cos\chi + k\cos 2\theta\sin\chi, \qquad & p_2 &= -r\sin 2\theta\sin\chi + k\cos 2\theta\cos\chi. \end{aligned} \tag{31}$$

As a result of the transformations performed, we obtain the system

$$\frac{dr}{d\tau} = -\frac{\tilde\gamma}{2}r - \varepsilon\eta\left(1+\frac{5}{8}(k^2+3r^2)\right)r + \frac{1}{16}\eta\left(r^2-k^2\right)\left(3k\sin 8\theta - 5\varepsilon r\cos 8\theta\right), \tag{32}$$

$$\frac{dk}{d\tau} = -\frac{\tilde\gamma}{2}k - \varepsilon\eta\left(1+\frac{5}{8}(3k^2+r^2)\right)k - \frac{1}{16}\eta\left(r^2-k^2\right)\left(3r\sin 8\theta - 5\varepsilon k\cos 8\theta\right), \tag{33}$$

$$\frac{d\theta}{d\tau} = -\frac{1}{4}\tilde v + \frac{3}{16}\eta kr\left(1+\cos 8\theta\right) + \frac{5}{32}\varepsilon\eta(k^2+r^2)\sin 8\theta, \tag{34}$$

$$\frac{d\chi}{d\tau} = -\frac{3}{16}\eta\left(r^2+k^2\right)\left(3+\cos 8\theta\right) - 10\varepsilon\eta kr\sin 8\theta. \tag{35}$$

In equations (32)–(35), all quantities are dependent on the precession angle θ, which is a consequence of using eight control sensors. Therefore, equations (32)–(35) do not allow for such a simple analysis as for the case of $n = 16$ electrostatic control sensors [15].

Using the change of variables (31), from (29) we obtain a system of equations in new variables for the case of $n = 16$ control sensors:

$$\frac{dr}{d\tau} = -\frac{\tilde\gamma}{2}r - \varepsilon\eta\left(1+\frac{5}{8}(k^2+3r^2)\right)r, \tag{36}$$

$$\frac{dk}{d\tau} = -\frac{\tilde\gamma}{2}k - \varepsilon\eta\left(1+\frac{5}{8}(3k^2+r^2)\right)k, \tag{37}$$

$$\frac{d\theta}{d\tau} = -\frac{1}{4}\tilde v + \frac{3}{8}\eta kr, \tag{38}$$

$$\frac{d\chi}{d\tau} = -\frac{9}{8}\eta\left(r^2+k^2\right). \tag{39}$$

Equations (36), (37) indicate that the oscillation amplitude decreases as a result of damping. Equation (39) indicates an insignificant change in the oscillation frequency. From (38) it follows that the angular velocity of the SSG drift is given by the formula

$$\dot\theta_* = \frac{3}{8}\eta kr. \tag{40}$$

From (36)–(39) it follows that taking into account the parameters of the electric control circuit for nonlinear oscillations of the resonator in the case of $n = 16$ control sensors has an insignificant effect on the damping of the oscillations and does not introduce changes in the angular velocity of the gyroscope drift. Thus, in the case of a SSG with $n = 16$ control sensors, there is a formula (38), which makes it possible to determine and take into account the angular velocity of the SSG drift, as well as to apply the classical force compensation technique, when the oscillation amplitude r is maintained constant, and k is sought to be reduced to zero [9].

Let us return to the analysis of the $n = 8$ control sensors case. In equations (32)–(35), despite their nonlinearity, it can be similarly noted that equations (32), (33) indicate a decrease in oscillation amplitude as a result of damping. Equation (35) indicates an insignificant change in oscillation frequency. Of greatest interest is equation (34), which yields an estimate of the angular velocity of the SSG drift:

$$-\frac{5}{32}\varepsilon\eta(k^2+r^2) \leqslant \frac{\mathrm{d}\theta_*}{\mathrm{d}\tau} \leqslant \frac{3}{8}\eta kr + \frac{5}{32}\varepsilon\eta(k^2+r^2). \tag{41}$$

According to (41), the angular velocity of the SSG drift is estimated by two fundamentally different terms. One of them is directly proportional to the amplitudes of the fundamental and quadrature oscillation waves r and k. Accordingly, with force compensation of the angular velocity of drift, when r is maintained constant and k is reduced to zero [9], this term, containing the product kr, is reduced to zero. However, with this standard compensation method, the angular velocity of drift estimated by the term in (41) containing $k^2 + r^2$ will not be compensated.

Let the quadrature k be completely compensated, $k = 0$. Then we will estimate the magnitude of the angular drift velocity:

$$\left|\frac{\mathrm{d}\theta_*}{\mathrm{d}\tau}\right| \leqslant \frac{5}{32}\varepsilon\eta r^2. \tag{42}$$

Thus, formulas (41) and (42) establish the presence of unavoidable drift of the SSG when using a SSG circuit with eight control sensors. It is obvious that, due to the high degree of smallness of ε, the unavoidable angular drift velocity is extremely small.

Neglecting ε in the estimate (41) and comparing it with formula (40), we find that the angular drift velocity of a SSG with eight control electrodes is estimated by the angular drift velocity of a SSG with sixteen control electrodes.

Example. Let's calculate the angular drift velocity of a SSG with a cylindrical quartz resonator, which is caused by the reference voltage when using $n = 8$ and $n = 16$ electrostatic control sensors.

The resonator has dimensions $R = 20$ mm, $H = R$, $h = 1$ mm, is made of quartz glass with a density $\rho = 2210$ kg/m^3, Young's modulus $E = 73.6$ GPa. With these parameters, the characteristic frequency of natural oscillations $\omega = 20890$ s^{-1} [14]. With a reference voltage $u_0 = 100$ V and a capacitance $C_0 = 1.05 \cdot 10^{-12}$ F, we have [14] $\eta = 9 \cdot 10^{-6}$, and $\varepsilon = 10^{-8}$.

We assume that the quadrature wave is fully compensated, $k = 0$, and the amplitude of the normalized fundamental wave is $r = 0.1$. Then, using the formula (42) for a SSG with $n = 8$ electrostatic control sensors, we obtain an estimate of the uncompensated angular drift velocity of $3 \cdot 10^{-12}$ s^{-1}, which is equal to $1.2 \cdot 10^{-6}$ °/hour. Such a small estimate of the angular drift velocity is insignificant even in high-precision gyroscopes, therefore a SSG with eight electrostatic control sensors is practically as accurate as a SSG with sixteen control sensors (this is only true for electrostatic control sensors with an extremely small parameter ε).

Otherwise, the angular drift velocity is compensated for as k approaches zero. [9]. Let us show that this compensation is necessary: let the relative amplitudes of the normalized fundamental and quadrature oscillation waves be $r = 0.1$ and $k = 0.001$ (respectively 10 microns and 0.1 microns), then the absolute value of the angular drift velocity, calculated by the formula (40), is equal to 1.45 °/hour. When using eight control sensors in the SSG, according to (41), the angular drift velocity is variable and is estimated by the calculated value 1.45 °/hour. The obtained value is significant for gyroscopes used in navigation systems, which indicates the manifestation of nonlinear properties of the control sensors and the need for compensation for the angular drift velocity in wave hemispheric gyroscopes.

2.2. Shift of the resonant peak of the amplitude-frequency characteristic. To study the amplitude-frequency characteristics of nonlinear oscillations, we will consider the following control

voltage supply mode: $u_1 = u_3 = u_4 = 0$, $u_2 = u$. Since the value of the parameter ε is extremely small, we will ignore it in this subsection and determine the most significant difference in the amplitude-frequency characteristics of the resonator oscillations using $n = 8$ and $n = 16$ control sensors. Since this study was conducted in [14] with $n = 16$ control sensors, we will consider the case of $n = 8$ control sensors here.

First, let us consider (14) only with cubic nonlinearity, without taking into account nonlinearity in control:

$$\begin{aligned} \frac{\mathrm{d}^2 f}{\mathrm{d}\tau^2} + f &= -\tilde{\gamma}\frac{\mathrm{d}f}{\mathrm{d}\tau} + \tilde{v}\frac{\mathrm{d}g}{\mathrm{d}\tau} + 2\eta f^3 + \eta u\cos\mu t, \\ \frac{\mathrm{d}^2 g}{\mathrm{d}\tau^2} + g &= -\tilde{\gamma}\frac{\mathrm{d}g}{\mathrm{d}\tau} - \tilde{v}\frac{\mathrm{d}f}{\mathrm{d}\tau} + 2\eta g^3. \end{aligned} \tag{43}$$

We will study the forced oscillations of the resonator in slow variables $A(\tau)$, $B(\tau)$, $\varphi(\tau)$, $\psi(\tau)$, which are the amplitudes and phases of the oscillations:

$$f = A\sin(\mu\tau + \varphi), \qquad g = B\sin(\mu\tau + \psi),$$

therefore we will use a change of variables

$$q_1 = A\sin\varphi, \quad p_1 = A\cos\varphi, \quad q_2 = B\sin\psi, \quad p_2 = B\cos\psi \tag{44}$$

in the averaged system with slow variables $q_1(\tau)$, $p_1(\tau)$, $q_2(\tau)$, $p_2(\tau)$. The corresponding system of averaged equations follows from (20) and by changing variables (44) is transformed into

$$\begin{aligned} \frac{\mathrm{d}A}{\mathrm{d}\tau} &= \frac{1}{2}\left[-\tilde{\gamma}A + \tilde{v}B\cos(\varphi - \psi) + \eta u\cos\varphi\right], \\ \frac{\mathrm{d}\varphi}{\mathrm{d}\tau} &= -\frac{1}{2A}\left[2A\lambda_* + \frac{3}{2}\eta A^3 + \tilde{v}B\sin(\varphi - \psi) + \eta u\sin\varphi\right], \\ \frac{\mathrm{d}B}{\mathrm{d}\tau} &= -\frac{1}{2}[\tilde{\gamma}B + \tilde{v}A\cos(\varphi - \psi)], \\ \frac{\mathrm{d}\psi}{\mathrm{d}\tau} &= -\frac{1}{2B}\left[2B\lambda_* + \frac{3}{2}\eta B^3 + \tilde{v}A\sin(\varphi - \psi)\right], \end{aligned} \tag{45}$$

where the frequency tuning $\lambda_* = \lambda/\omega$.

One of the stationary oscillation modes is the [23] mode with zero amplitude $B = 0$. Then from (45) follow the equations for determining the amplitude A and the oscillation phase φ:

$$\begin{aligned} &-\tilde{\gamma}A + \eta u\cos\varphi = 0, \\ &A\left(2\lambda_* + \tfrac{3}{2}\eta A^2\right) + \eta u\sin\varphi = 0. \end{aligned} \tag{46}$$

By eliminating the trigonometric functions in the equations (46), we obtain the expression

$$A^2\tilde{\gamma}^2 + \left(2\lambda_* A + \frac{3}{2}\eta A^3\right)^2 = \eta^2 u^2. \tag{47}$$

Applying the formula for differentiating an implicit function to (47), we write the condition for the extremum of $A(\lambda_*)$:

$$\frac{4A\left(2\lambda_* A + \dfrac{3}{2}\eta A^3\right)}{2A\tilde{\gamma}^2 + \left(2\lambda_* A + \dfrac{3}{2}\eta A^3\right)\left(2\lambda_* + \dfrac{9}{2}\eta A^2\right)} = 0,$$

from which it follows that $A(\lambda_*)$ has an extremum at the point

$$\lambda_* = -\frac{3}{4}\eta A^2. \tag{48}$$

Substituting (48) into expression (47), we determine the maximum value of the amplitude

$$A_{\max} = \frac{\eta u}{\tilde{\gamma}}, \tag{49}$$

taking into account which in (48), we obtain the value of the frequency tuning:

$$\lambda_{*\max} = -\frac{3\eta}{4}\left(\frac{\eta u}{\tilde{\gamma}}\right)^2. \tag{50}$$

Thus, when describing resonator oscillations using a nonlinear mathematical model that takes into account only cubic nonlinearity, the maximum oscillation amplitude is given by formula (49), and a leftward shift of the resonant oscillation peak is observed, according to formula (50), which corresponds to the description of oscillations with a soft characteristic.

Comparing the obtained results with a similar study for the case of $n = 16$ control sensors [14], the maximum amplitude in both cases is equal to (49), and the resonant peak shift for a SSG with sixteen control electrodes [14] is one and a half times greater.

$$\lambda_{*\max} = -\frac{9\eta}{8}\left(\frac{\eta u}{\tilde{\gamma}}\right)^2, \tag{51}$$

than for a SSG with eight control electrodes (50).

Let us now consider a nonlinear mathematical model that takes into account not only cubic nonlinearity, but also quadratic nonlinearity in control in the case of $n = 8$ control sensors. Similar to the above, from (20) with the change of variables (44) we obtain

$$\begin{aligned}
\frac{dA}{d\tau} &= \frac{1}{2}\left[-\tilde{\gamma}A + \tilde{v}B\cos(\varphi-\psi) + \eta u\left(1+\frac{3}{4}A^2\right)\cos\varphi\right],\\
\frac{d\varphi}{d\tau} &= -\frac{1}{2A}\left[2A\lambda_* + \frac{3}{2}\eta A^3 + \tilde{v}B\sin(\varphi-\psi) + \eta u\left(1+\frac{9}{4}A^2\right)\sin\varphi\right],\\
\frac{dB}{d\tau} &= -\frac{1}{2}[\tilde{\gamma}B + \tilde{v}A\cos(\varphi-\psi)],\\
\frac{d\psi}{d\tau} &= -\frac{1}{2B}\left[2B\lambda_* + \frac{3}{2}\eta B^3 + \tilde{v}A\sin(\varphi-\psi)\right].
\end{aligned} \tag{52}$$

We consider the stationary oscillation mode with $B = 0$ and obtain an expression for the resonance curve:

$$\left(A\tilde{\gamma}\left(1+\frac{9}{4}A^2\right)\right)^2 + \left(A\left(2\lambda_* A + \frac{3}{2}\eta A^3\right)\left(1+\frac{3}{4}A^2\right)\right)^2 = \left(\eta u\left(1+\frac{9}{4}A^2\right)\left(1+\frac{3}{4}A^2\right)\right)^2. \tag{53}$$

Thus, the resulting analytical expression (53) describes the amplitude-frequency characteristics of oscillations, taking into account both cubic nonlinearity and quadratic nonlinearity in control.

Applying the implicit function differentiation formula to (53), we obtain the extremum condition for $A(\lambda_*)$, from which it follows that $A(\lambda_*)$ has an extremum at the point $\lambda_* = -\frac{3}{4}\eta A^2$. Substituting the obtained value of λ_* into (53), we determine the maximum amplitude:

$$A_{\max} = \frac{2\tilde{\gamma}}{3\eta u}\left(1 - \sqrt{1 - 3\left(\frac{\eta u}{\tilde{\gamma}}\right)^2}\right). \tag{54}$$

If in (54) we use the Taylor series expansion, accepting the constraint $\frac{\eta u}{\tilde{\gamma}} < 1$, caused by the breakdown-free operation of electrostatic sensors (which is true according to formula (49)), then we arrive at a refinement of the value of the maximum amplitude (49) by taking into account the nonlinearity in control:

$$A_{\max} = \frac{2\tilde{\gamma}}{3\eta u}\left(1 - \left(1 - \frac{3}{2}\left(\frac{\eta u}{\tilde{\gamma}}\right)^2 - \frac{9}{8}\left(\frac{\eta u}{\tilde{\gamma}}\right)^4 - \frac{27}{16}\left(\frac{\eta u}{\tilde{\gamma}}\right)^6 - \dots\right)\right) = \frac{\eta u}{\tilde{\gamma}} + \frac{3}{4}\left(\frac{\eta u}{\tilde{\gamma}}\right)^3 + \frac{9}{16}\left(\frac{\eta u}{\tilde{\gamma}}\right)^5 + \dots. \tag{55}$$

Taking into account the refined value of the maximum amplitude, we calculate the refined value of the frequency tuning:

$$\lambda_{*\max} = \eta - \frac{2\tilde{\gamma}^2}{3u^2\eta}\left(1 - \sqrt{1 - 3\left(\frac{\eta u}{\tilde{\gamma}}\right)^2}\right). \tag{56}$$

To see the refinement of the resonant frequency caused by taking into account the quadratic nonlinearity in control, and compare with (50), we expand (56) in a series

$$\lambda_{*\max} = \eta - \frac{2\tilde{\gamma}^2}{3u^2\eta}\left(\frac{3}{2}\left(\frac{\eta u}{\tilde{\gamma}}\right)^2 + \frac{9}{8}\left(\frac{\eta u}{\tilde{\gamma}}\right)^4 + \frac{27}{16}\left(\frac{\eta u}{\tilde{\gamma}}\right)^6 + \dots\right) =$$

$$= -\frac{3}{4}\eta\left(\frac{\eta u}{\tilde{\gamma}}\right)^2 - \frac{9}{8}\eta\left(\frac{\eta u}{\tilde{\gamma}}\right)^4 - \dots . \tag{57}$$

From formulas (49), (55) it follows that the oscillation amplitude increases as a result of taking into account the quadratic nonlinearity in control, which leads, according to formulas (50), (57), to a greater shift in the resonant peak of the soft amplitude-frequency characteristic.

For a SSG with sixteen control electrodes, an expression for the resonant curve was obtained in [14]

$$\left(A\tilde{\gamma}\left(1 + \frac{9}{4}A^2\right)\right)^2 + \left(A\left(2\lambda_* A + \frac{9}{4}\eta A^3\right)\left(1 + \frac{3}{4}A^2\right)\right)^2 =$$

$$= \left(\eta u\left(1 + \frac{9}{4}A^2\right)\left(1 + \frac{3}{4}A^2\right)\right)^2 \tag{58}$$

and the corresponding formulas were derived:

$$A_{\max} = \frac{2\tilde{\gamma}}{3\eta u}\left(1 - \sqrt{1 - 3\left(\frac{\eta u}{\tilde{\gamma}}\right)^2}\right), \quad \lambda_{*\max} = \frac{3\eta}{2} - \frac{\tilde{\gamma}^2}{u^2\eta}\left(1 - \sqrt{1 - 3\left(\frac{\eta u}{\tilde{\gamma}}\right)^2}\right). \tag{59}$$

From (54), (56), (59) it follows that the maximum amplitude $A_{\max}$ is the same in the case of using both eight and sixteen control electrodes, and the shift of the resonance peak for a SSG with sixteen control electrodes is one and a half times greater than for a SSG with eight control electrodes.

Example. Let us construct the amplitude-frequency characteristics of the oscillations of a cylindrical resonator of a SSG with eight and sixteen electrostatic control sensors. As in the previous numerical example, we take the data $\omega = 20890\ \text{s}^{-1}$, $\eta = 9 \cdot 10^{-6}$, $u = 0.1$, and adopt the quality factor $Q = 5 \cdot 10^5$. We perform the calculations using formulas (53) and (58). In Fig. 1 plots the amplitude-frequency characteristics calculated according to (53) and (58); the normalized oscillation amplitude A is plotted along the vertical axis, and the frequency tuning λ is plotted along the horizontal axis.

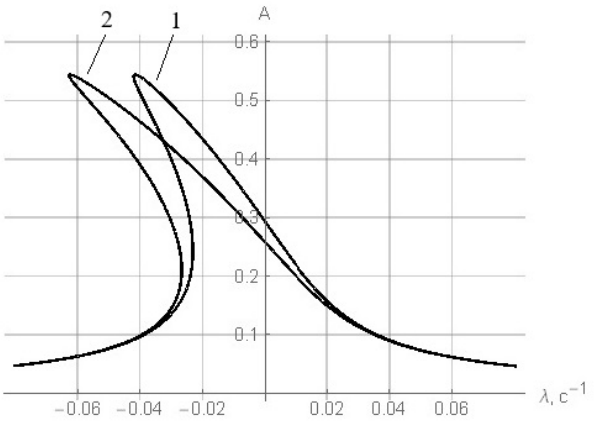

Fig. 1. Amplitude-frequency response: 1— for gyroscope with eight control sensors, 2— for gyroscope with sixteen control sensors

According to formulas (54) and (56) we obtain the values $A_{\max} = 0.544$ and $\lambda_{\max} = -0.0415\ \text{s}^{-1}$ for a SSG with eight control electrodes, and, accordingly, according to formulas (59) $A_{\max} = 0.544$ and $\lambda_{\max} = -0.0623\ \text{s}^{-1}$ for a SSG with sixteen control electrodes.

2.3. Discussion of results. In accordance with the statement about the need to take into account the specifics of a particular oscillatory system when studying the nonlinearity of oscillations [9],

it is shown that the nonlinearity of the oscillations of the SSG resonator caused by electrostatic control sensors depends on the number of control sensors.

Previously, in [14], the dynamics of a SSG resonator with only sixteen control sensors was investigated, and the result was a special cubic nonlinearity of $\left(f^2+g^2\right)f$ and $\left(f^2+g^2\right)g$ in the equations (26), characteristic of gyroscopes of the generalized Foucault pendulum class [9] and also derived in [23] for a SSG under the assumption that the resonator material obeys a nonlinear elasticity law. This type of nonlinearity led to a constant angular drift velocity (40). In [14] this type of nonlinearity caused by electrostatic control sensors was called a nonlinear refinement of the well-known "negative electrostatic stiffness"effect, which can be easily seen from the equations (26): in the first equation, the terms $\left(1-2\eta-3\eta\left(f^2+g^2\right)\right)f$ can be grouped, and in the second, the terms $\left(1-2\eta-3\eta\left(f^2+g^2\right)\right)g$.

This paper shows that the use of eight control sensors leads to a completely different type of cubic nonlinearity of f^3 and g^3 in equations (14). The resulting cubic nonlinearity cannot be attributed to the "negative electrostatic stiffness"effect and leads to a variable angular drift velocity, which can only be estimated (41). This circumstance significantly complicates the calculations of the angular velocity and excludes the possibility of analytical compensation for the angular drift velocity, but, on the other hand, does not affect the force compensation for the angular drift velocity based on the suppression of the quadrature oscillation wave [9].

Also in this paper, consideration is given to terms containing the small parameter ε, which characterizes the electrical oscillation control circuit. It is shown that for SSG with eight electrostatic control sensors, an unavoidable angular drift velocity (42) occurs, which is negligible even for high-precision gyroscopes. At the same time, [15] showed the complete absence of an irreversible angular drift velocity for SSG with sixteen control sensors.

In the work [24] it is shown that the electrical balancing of the SSG resonator using eight control electrodes, in contrast to the SSG with sixteen control sensors, does not allow for full compensation of frequency differences.

On the other hand, this study demonstrates that the nonlinear effects of resonator dynamics in a SSG with eight control sensors are weaker than in a SSG with sixteen control sensors: the variable angular drift velocity is smaller than the constant velocity that occurs when using sixteen control sensors, and the shift in the resonant peak of the oscillation amplitude-frequency response is one and a half times smaller. It is also important to consider the practical benefits of using eight control sensors: halving the number of control sensors simplifies the device design and reduces the cost of manufacturing.

Thus, it can be concluded that a SSG with eight electrostatic control sensors offers advantages in terms of ease of manufacture and reduced nonlinear effects of resonator dynamics compared to a SSG with sixteen control sensors. However, when developing a SSG (especially a high-precision one), it is necessary to consider the risks of using a SSG with eight control sensors: electrical balancing is ineffective in this SSG design, calculating the angular drift velocity is significantly difficult due to its variable value, and there is an inherent angular drift velocity, which depends on the smallness of the parameter characterizing the electrical oscillation control circuit.

Conclusion

Nonlinear mathematical models of the dynamics of a cylindrical resonator of a wave solid-state gyroscope are constructed. These models take into account the nonlinearities caused by the excitation of oscillations by electrostatic control sensors for eight and sixteen control sensors. For these cases, differences in the nonlinearities in the differential equations are demonstrated, as well as differences in the nonlinear effects of the resonator dynamics of the wave solid-state gyroscope: in the angular drift velocity and in the shift of the resonant peak of the amplitude-frequency response. Nonlinear effects are more pronounced in the case of a wave solid-state gyroscope with sixteen control sensors; the angular drift velocity and the shift of the resonant peak of the amplitude-frequency response are greater than for a wave solid-state gyroscope with eight control sensors. However, in the case of a wave solid-state gyroscope with eight control sensors, the angular drift velocity is variable and also contains a small uncompensated component. The effects discovered for the SSG circuit with eight electrostatic control sensors are of theoretical significance, but do not affect the practical use of such SSG due to the same procedure of force compensation for both

constant and variable angular drift velocity and the high order of smallness of the uncompensated angular drift velocity.

References

1. Perelyaev S.E. Review and analysis of the lines of development of strapdown inertial navigation systems on the basis of hemispherical resonator gyroscopes. Navigation News. 2018;(2):21–27 (in Russian).
2. Perelyaev S.E. Current State of Wave Solid-State Gyroscopes. Development Prospects in Applied Gyroscopy. In: Proc. of 30th Saint Petersburg International Conference on Integrated Navigation Systems. 2023. 29–31 May 2023, Saint Petersburg, Russian Federation. P. 1–4. DOI: 10.23919/ICINS51816.2023.10168310.
3. Peshekhonov V.G. The outlook for gyroscopy. Gyroscopy Navig. 2020;11(3):193–197. DOI: 10.1134/S2075108720030062.
4. Maslov A.A, Maslov D.A, Merkuryev I.V. Nonlinear effects in the dynamics of HRG with flat electrodes. Gyroscopy Navig. 2023;14(4):320–327. DOI: 10.1134/S2075108724700044.
5. Zhuravlev V.Ph, Klimov D.M. Wave Solid-State Gyroscope. M.: Nauka; 1985. 125 p. (in Russian).
6. Zhuravlev V.Ph, Klimov D.M, Zbanov Yu.K. Quartz Hemispherical Resonator (Wave Solid-State Gyroscope). M.: Kim L.A.; 2017. 194 p. (in Russian).
7. Zhuravlev V.Ph. Theoretical foundations of solid-state wave gyroscopes. Mech. Solids. 1993;28(3): 3–15.
8. Zhuravlev V.Ph. Global evolution of state of the generalized Foucault pendulum. Mech. Solids. 1998;33(6):3–8.
9. Zhuravlev V.Ph. A controlled Foucault pendulum as a model of a class of free gyros. Mech. Solids. 1997;32(6):21–28.
10. Zhuravlev V.Ph, Lynch D.D. Electric model of a hemispherical resonator gyro. Mech. Solids. 1995; 30(5):10–21.
11. De S.K, Aluru N.R. Complex nonlinear oscillations in electrostatically actuated microstructures. Journal of Microelectromechanical Systems. 2006;15(2):355–369. DOI: 10.1109/JMEMS.2006.872227.
12. Rhoads J.F, Shaw S.W, Turner K.L, Moehlis J, DeMartini B.E, Zhang W. Generalized parametric resonance in electrostatically actuated microelectromechanical oscillators. Journal of Sound and Vibration. 2006;296(4-5):797–829. DOI: 10.1016/j.jsv.2006.03.009.
13. Maslov A.A, Maslov D.A, Merkuryev I.V. Nonlinear effects in dynamics of cylindrical resonator of wave solid-state gyro with electrostatic control system. Gyroscopy Navig. 2015;6: 224–229. DOI: 10.1134/S2075108715030104.
14. Maslov D.A, Merkuryev I.V. Impact of nonlinear properties of electrostatic control sensors on the dynamics of a cylindrical resonator of a wave solid-state gyroscope. Mech. Solids. 2021;56(6): 960–979. DOI: 10.3103/S002565442106011X.
15. Maslov D.A. Nonlinear dynamics of a wave solid-state gyroscope taking into account the electrical resistance of an oscillation control circuit. Rus. J. Nonlin. Dyn. 2023;19(3):409–435. DOI: 10.20537/nd230602.
16. Lunin B.S, Basarab M.A, Yurin A.V, Chumankin E.A. Fused quartz cylindrical resonators for lowcost vibration gyroscopes. In: Proc. of 25th Saint Petersburg International Conference on Integrated Navigation Systems (ICINS). 28–30 May 2018, St. Petersburg, Russia. P. 1–4. DOI: 10.23919/ICINS.2018.8405896.
17. Lunin B.S, Lopatin V.M. Silica glass for high-Q mechanical resonators. Inorg. Mater. 2020;56: 292–296. DOI: 10.1134/S0020168520030103.
18. Wu X, Xi X, Wu Y, Xiao D. Cylindrical Vibratory Gyroscope. Singapore: Springer; 2021. 202 p. DOI: 10.1007/978-981-16-2726-2.
19. Zeng L, Luo Y, Pan Y, Jia Y, Liu J, Tan Z, Yang K, Luo H. Million quality factor cylindrical resonator with improved structural design based on thermoelastic dissipation analysis.

Sensors. 2020;20(21):6003. DOI: 10.3390/s20216003.
20. Tao Y, Pan Y, Liu J, Jia Y, Yang K, Luo H. A novel method for estimating and balancing the second harmonic error of cylindrical fused silica resonators. Micromachines. 2021;12(4): 380. DOI: 10.3390/mi12040380.
21. Maslov A.A, Maslov D.A, Merkuryev I.V. Studying stationary oscillation modes of the gyro resonator in the presence of positional and parametric excitations. Gyroscopy Navig. 2014;5: 224–228. DOI: 10.1134/S2075108714040099.
22. Zhuravlev V.Ph, Klimov D.M. Applied Methods in Vibration Theory. M.: Nauka; 1988. 328 p. (in Russian).
23. Merkuryev I.V, Podalkov V.V. Dynamics of Micromechanical and Wave Solid-State Gyroscopes. M.: Fizmatlit; 2009. 228 p. (in Russian).
24. Maslov A.A, Maslov D.A, Merkuryev I.V. Electrical Balancing of Wave Solid-State Gyroscope with Flat Electrodes. In: Proc. of 31th Saint Petersburg International Conference on Integrated Navigation Systems. 2024. P. 313–316.